HHS Public Access

Author manuscript

Obesity (Silver Spring). Author manuscript; available in PMC 2017 January 30.

Published in final edited form as:

Obesity (Silver Spring). 2010 December ; 18(12): 2379–2384. doi:10.1038/oby.2010.48.

Quantification of intermuscular adipose tissue in the erector spinae muscle by MRI: agreement with histological evaluation of lipid

Andrea Rossi, **Elena Zoico**, **Bret H Goodpaster**, **Anna Sepe**, **Vincenzo Di Francesco**, **Francesco Fantin**, **Francesca Pizzini**, **Francesca Corzato**, **Alessandra Vitali**, **Rocco Micciolo**, **Tamara B Harris**, **Saverio Cinti**, and **Mauro Zamboni**

Division of Geriatric Medicine, University of Verona, Verona, Italy (AR, EZ, AS, VDF, FF, FC, MZ); Division of Endocrinology and Metabolism, Department of Medicine, University of Pittsburgh (BHG); the Service of Neuroradiology, Borgo Trento Hospital, Verona, Italy (FP); Institute of Normal Human Morphology and Anatomy, University of Ancona, Italy (AV, SC), Department of Statistics, University of Trento, Italy (RM); the Laboratory of Epidemiology, Demography and Biometry, Geriatric Epidemiology Section, National Institute of Aging, Bethesda, MD, USA (TBH)

Abstract

Deposition of fat between skeletal muscle bundles and beneath the muscle fascia, recently called intermuscular adipose tissue (IMAT), is gaining attention as potential contributor to insulin resistance, metabolic syndrome, muscle function impairment and disability.

The aim of this study was to compare IMAT as measured at the erector spinae level by MRI, a well-recognized gold standard method to evaluate fat content inside muscles, and histology estimates.

In 18 healthy elderly men and women with a wide range of BMI (25.05–35.58 Kg/m^2), undergoing elective vertebral surgery, IMAT within the erector spinae muscle was evaluated by MRI, by body composition using dual energy x-ray absorptiometry and histological evaluation of intraoperative biopsy sample.

The concordance between IMAT/TA ratio evaluated by MRI and histological examination was analyzed employing Lin's concordance correlation coefficient and the procedure proposed by Bland and Altman. Two threshold to distinguish between muscle and IMAT calculated respectively by 20% and 10% reduction of the gray level intensity evaluated by MRI from surrounding subcutaneous adipose tissue were used. With a 20% reduction, calculated IMAT/TA as evaluated by MRI on average exceeds histological evaluation by 21.79%, whereas by reducing the threshold by 10% agreement between MRI and histology improved with a 12.42% difference.

Our data shows a good degree of concordance between IMAT assessment by magnetic resonance and histology and seems to show that agreement between the two methods could be improved by using a more restrictive threshold between muscle and fat.

Correspondence and reprint requests to: Mauro Zamboni, MD, Dipartimento Scienze Biomediche e Chirurgiche, Sezione di Geriatria, Ospedale Maggiore, P.le A. Stefani 1, 37126 Verona - ITALY, +39-045-8072537, +39-045-8072043 (fax), mauro.zamboni@univr.it.

Keywords

IMAT; body composition; MRI; adipocyte

INTRODUCTION

Deposition of fat between skeletal muscle bundles and beneath the muscle fascia, recently identified as intermuscular adipose tissue (IMAT), is gaining attention as potential contributor to insulin resistance and metabolic syndrome (1–3). Histologically IMAT is considered to be primarily adipose tissue, mainly composed of adipocytes, located between muscle fibers, also known as extramyocellular lipids, not including that located within muscle fibers in form of cytosolic triacylglycerols, known as intramyocellular lipids (4). It has been observed that the amount of IMAT as evaluated at the thigh level by computed tomography (CT) is directly and strongly associated with age, adiposity (3) and muscle function impairment (5).

Whole body IMAT has also been measured using magnetic resonance imaging (MRI) and has been shown to increase with age, even in weight-stable elderly women over a 2-year period of follow-up (6). Imaging methods, such as computed tomography (CT) and magnetic resonance imaging (MRI), are considered the most accurate methods available for in vivo quantification of body composition at the tissue-organ level, especially for human studies. In particular CT and MRI are considered the gold standard methods to measure intermuscular adipose tissue in vivo (2,6,7).

The accuracy of arm and leg MRI and CT IMAT estimates with corresponding cadaver estimates has been shown (8). However, no studies have compared the accuracy of MRI measurement of muscle tissue composition with corresponding histology in vivo. In particular no information is available on the comparison between MRI IMAT evaluation measured within erector spinae musculature and histology evaluation, despite the suggestion that IMAT increase with age in these muscles, infiltrating characteristically around the posterior aspect of the vertebral bodies (9).

The aim of this study was to compare the degree of lipid infiltration of the muscle, expressed as a ratio between IMAT and total muscle area, including IMAT interspersed between muscle fibers, as measured at the erector spinae level by MRI, a well-recognized gold standard method to evaluate fat content inside muscles, and histology estimates of adipocyte area from biopsy samples of these muscles, which are known to have a greater age-related lipid infiltration than other groups of muscles (9). Furthermore, evaluation of biopsies taken during surgery and not carried out with percutaneous needle biopsy at the level of the vastus lateralis, result in larger and more representative samples of the original appearance of the tissue.

We also tested whether the use of alternative threshold signal intensity than the 20% reduction of subcutaneous adipose tissue (SAT) lipid signal previously used by Song et al (6) to distinguish between muscle and IMAT, could improve the agreement between the two measurements.

METHODS AND PROCEDURES

A total of 13 men and 5 women, aged between 58 and 81 years, with BMI ranging from 25.05 to 35.58 Kg/m^2, were studied.

All subjects were selected among those undergoing elective surgery for medullar lumbar stenosis in the Department of Neurosurgery of our Hospital.

All subjects had been in good general health, as determined by a complete medical history and physical examination, as well as a normal blood count, chemical screening battery, and urine analysis. All individuals had been weight-stable over the previous 6 months and had no evidence of cancer, liver, renal, thyroid, chronic inflammatory diseases, chronic heart failure (New York Heart Association class 3 or higher), or serious lung disease. Moreover, subjects with previous diagnosis of type 2 diabetes were excluded. Patients receiving steroid, pain and/or immunosuppressive medications either locally or systemically in the previous six months were not considered eligible for the study. None of the subjects received insulin, thiazolidinediones, any hypoglycemic or lipid lowering drug nor was using anti-inflammatory medications.

None of the participants was regularly engaged in physical activity.

All participants gave their informed consent and the Ethical Committee of the University Hospital of Verona approved the experimental protocol.

Anthropometry

With the subjects wearing light clothes and no shoes, body weight was measured to the nearest 0.1 Kg (Salus scale, Milan, Italy), and height to the nearest 0.5 cm using a audiometer (Salus stadiometer, Milan, Italy). BMI was computed as weight divided by stature squared (Kg/m^2). Waist circumference was obtained with a measuring tape at the level of the narrowest part of the torso, as seen from the front.

Dual energy X-ray Absorptiometry (DXA)

Body composition was studied using Dual energy X-ray absorptiometry (DXA) (Hologic QDR 4500, Waltham, USA) fan beam with software version 8.21 (10). Total body fat (FM) was expressed in Kg as well as a percentage of body weight (FM %). Lean body mass (LBM) was considered as the difference between fat-free mass (FFM) and bone mineral mass and expressed in Kg. Compartments of arms and legs were also examined, using the sub-region option of the software. Appendicular skeletal muscle mass (ASMM) was calculated as the sum of arms and legs lean soft-tissue masses.

The CV for double determinations performed on the same day, in 10 subjects (male and female aged 65–75 years), with subjects repositioned in between scans, was 1% for FM and 1.3% for LBM and ASMM.

Study of muscle fat infiltration with MRI

Subjects were positioned supine on a MR scanner and the imaging protocol took about 6 minutes per subject. Transverse sections were obtained at L3–L4 disk level using a 1.0-T Siemens Armony Expert (Siemens AG, Erlangen, Germany), with a surface coil. A high resolution T1-weighted sequence was obtained for every subject. The scanning parameters for this sequence were TR 450, TE 15, Matrix 512×512, FOV 240mm, GAP 0.4mm, Averages 3, Scan time 5.48s, Voxel Size 0.8×0.5×4.0mm.

Erector spinae measurements (including the multifidus, longissimus and iliocostalis) at the L3–L4 disc level on the right and left side were selected for the analysis because the erector spinae cross sectional area have previously been found to be largest overall at this level (11,12). The side corresponding to biopsy sampling was considered for imaging analyses.

A single trained reader (AR) analyzed all the L3–L4 images using Sliceomatic image analysis software (version 4.2; Tomovision, Montreal, Canada) and measured total area (TA) and IMAT of the left and right erector spinae muscle. IMAT was defined as adipose tissue area visible between muscle groups and beneath the muscle fascia.

A well-established nonparametric nonuniform intensity normalization (N3) algorithm was used to correct smoothly varying shading caused by poor radiofrequency coil uniformity or gradient-driven eddy currents (13) prior to analysis for IMAT.

The gray level intensity (threshold value) of the adipose tissue in the subcutaneous adipose tissue (SAT) region was determined in agreement with Song et al (6). This value was reduced by 20% to identify the erector spinae IMAT threshold (6); then alternatively, we used a gray level intensity reduction of 10% of the surrounding SAT to quantify IMAT in order to test if this different threshold could improve agreement between MRI and histology.

Muscle area (MA) was considered as the difference between TA and IMAT; the IMAT/TA ratio, was also calculated.

Erector spinae muscle biopsies: fat infiltration quantification

Human Subjects—Multifidus muscle biopsies were taken at the beginning of vertebral surgery in the site of surgical incision (L3–L4), in a standardized manner (maximum 30 minutes after the induction of anesthesia with the same type of anesthetic drugs). None of the patients studied had previous vertebral surgery before, nor other types of surgical scares in the site of surgical incision.

Light microscopy—Tissue biopsies were fixed by immersion in 4% paraformaldehyde in 0.1M phosphate buffer, pH 7.4 overnight at 4°C, dehydrated, cleared and paraffin embedded. 3μm thick sections from three different levels (every 200μm) were cut to obtain sections representative of the whole biopsy.

All sections were stained with Hematoxilin and Eosin (H&E) for histological and morphometric analysis.

The morphological observations were performed with a Nikon Eclipse 80i light microscopy (Nikon, Japan).

Morphometry—For each patient the three level sections of M, H&E stained, were used for the measurement of area occupied by adipose tissue infiltration in muscle as previously reported with more precise indication in this study derived by immunostaining with perilipin antibody (14–17).

The images of the whole section in every slide were captured with a Nikon DXM 1200 camera at 10× magnification. In every image, the area of adipose infiltration and the total area (TA = adipocyte area + muscle) were drawn and measured using an image analysis software (Lucia Image v.4.82, Nikon Instruments, Cz).

Results are given as % of adipocyte area/TA ratio of the three levels (Histology adipocyte area/TA). The mean of % adipocyte area/TA of the three different levels was used. The intraclass correlation coefficients for % adipocyte area/TA at the three different levels was 0.908 (95% CI 0.793–0.964).

The areas of fibrosis containing perilipin negative isolated lipid droplets of different sizes have been calculated in a random subsample of 5 subjects (3 men and 2 women, mean age 71.2 ± 10.3 years, mean BMI 30.76 ± 6.9 Kg/m2). The mean values for the perilipin negative area were 10.95 ± 2.72 % with a range between 7.88 and 15.45.

Immunohistochemistry—3μm thick de-waxed sections were incubated according to the Avidin-Biotin Peroxidase Complex method (ABC) following these steps: 1) 3% hydrogen peroxide to inactivate endogenous peroxidase; 2) normal goat serum (1:75) to reduce non specific background; 3) rabbit anti-perilipin (kindly provided by A. Greenberg, Boston) at 1:300 dilution, 4°C overnight; 4) goat anti rabbit IgG biotin – conjugated, 1:200 (Vector Labs, Burlingame, CA); 5) ABC complex (Vector Labs, Burlingame, CA); 6) enzymatic visualization with Sigma Fast as cromogen. Method specificity tests were performed with the omission of the primary antibody. Sections were counterstained with hematoxylin and finally mounted in Eukitt (Fluka Germany).

Statistical analysis

Results are shown as mean ± SD unless otherwise stated. The Pearson correlations were used to test associations between variables.

The concordance between IMAT/TA ratio evaluated by MRI and by histological examination was analyzed employing the Lin's concordance correlation coefficient (18) and the procedure proposed by Bland and Altman (19).

The level for statistical significance was $p<0.05$ for all the variables. All statistical analyses were performed using the SPSS statistical package 13.0 for Windows (20).

RESULTS

Table 1 shows the main characteristics of the study sample.

Intra-rater reliability estimates of muscle composition measurements were based on MR images of 10 randomly selected men (mean age 68.1 y, mean BMI 29.44 kg/m^2) evaluated twice, 4–8 weeks apart. The subjects MR images were placed in a random order for the second evaluation and the measurer was blinded to the results of the first session. Intraclass Correlation Coefficient was 0.983 for TA, 0.985 for MA, 0.974 for IMAT and 0.982 for IMAT/TA.

Table 2 shows the associations between age, anthropometric measures, body composition, MRI measurements and histology in the whole study sample.

Association between IMAT/TA as evaluated by histology and IMAT/TA ratio as evaluated by MRI with 20% and 10% reduction of the gray level intensity referenced from the surrounding SAT are presented respectively in Figure 1A and 1B. The Pearson correlation coefficients were, respectively, 0.792 and 0.843. However, to evaluate the degree of concordance between MRI and histology we quantified how much the two readings fall on the 45° line through the origin. In such a case, the Lin's concordance correlation coefficients yields different results, the correlation being 0.299 and 0.490, respectively. Such lack of concordance was mostly due to a bias in MRI procedure quantified according to Bland and Altman.

Figure 2A and 2B plots differences between IMAT/TA measured by MRI respectively with 20% and 10 % reduction of the gray-level intensity referenced from the surrounding SAT and adipocyte area evaluated by histology. The Bland-Altman plots are summarized by the mean difference (IMAT/TA as evaluated by MRI on average exceed histological evaluation by 21.79 % with 95% confidence interval 17.54 to 26.05 and by 12.42 % with 95% confidence interval 9.27 to 15.24, respectively with 20% and 10 % reduction of the SAT gray-level intensity). However, the correlation between IMAT/TA ratio and means was not significant for both (respectively $r=0.36$, $p=0.146$ and $r=-0.17$, $p=0.500$).

If we correct for the bias shown by the Bland-Altman plots subtracting 21.79 from all IMAT/TA MRI readings with 20% reduction of the SAT gray-level intensity (or, respectively, subtracting 12.42 from all IMAT/TA MRI readings with 10% reduction of the SAT gray-level intensity) the concordance with histology increases; in fact Lin's concordance correlation coefficients become 0.771 and 0.839 respectively. Light microscopy showed that areas of fibrosis containing perilipin negative isolated lipid droplets of different sizes occupied about 8–15% of each histology section examined (Figure 3).

DISCUSSION

Our data shows a good degree of concordance between IMAT assessment by magnetic resonance and histology.

Both MRI and histology IMAT were significantly positively related to BMI, waist and negatively associated with MA.

No other study has determined the direct association between adipose tissue between muscle fibers as evaluated by histology and intermuscular adipose tissue measured by magnetic resonance.

It has been previously shown that lipid contained within muscle fibers as determined with histochemical staining of lipid was negatively associated with muscle attenuation as evaluated by CT suggesting that muscle attenuation varies as a function of muscle lipid content (21) with a relatively similar level of agreement. However, CT IMAT has not been compared with histology. The accuracy of arm and leg MRI and CT IMAT estimates with corresponding cadaver estimates has been previously described (8). In this comparative study MRI images were matched with corresponding photographs of the cadaver anatomical sections at the semifrozen state with technical problems due to inadequate contrast between muscle and adipose tissue, and microscopic evaluation of adipose tissue was not taken into account. Comparison of MRI with corresponding two cadaver analysis of leg and arm sections showed a high correlation ($r=0.92$, $p<0.001$) for IMAT.

Our data shows that percentage fat infiltration in muscle, as evaluated by MRI, considering 20% reduction of the gray level intensity referenced from the surrounding SAT to distinguish the threshold between muscle and IMAT signal intensity as suggested by Song et al, was higher than the percentage measured by histology with a mean difference of 21.79%. Considering 10% reduction of the grey level intensity referenced from the surrounding SAT an improvement in the association between the two measurements was observed, with a 12.42% difference between the two methods. Although the IMAT/TA ratio evaluated by MRI was significantly associated with histological measurement explaining 63% up to 82% of its variance, depending on the threshold between IMAT and muscle used, it was biased, with an overestimation of percent IMAT/TA on MRI as shown by the Bland Altman plot in Figure 2A and 2B. However, this finding is not unexpected for several reasons. First, extrapolation of intermuscular adipose tissue contained within transverse sections representative of whole erector spine biopsy to the intermuscular adipose tissue content of whole muscle on a cross-sectional MRI image is difficult, particularly because variability in the lipid content in different transverse section samples from the same individual is quite high. However, this does not seem to be relevant at least in our study as mean differences among the three histology evaluations are small and not significant. Second Hematoxilin and Eosin (H&E) used to stain histological section for morphometric analysis and the use of anti-perilipin antibody allow to distinguish adipocytes (perilipin positive) but not isolated lipid droplets in the interstitial space among muscle fibers. The rough estimation that 8–15% of the sectional area of biopsies was occupied by perilipin negative lipid droplets of various sizes could partially account of the observed difference between MRI and histology. Moreover, if we correct for this bias, the degree of concordance, as quantified by Lin’s concordance correlation coefficient, increases significantly.

It is also true that although we used the subcutaneous adipose tissue distribution of values to determine IMAT within the area of the muscle as has been previously suggested (6), this method lacks the precision of the histology. However, changing the threshold for distinguishing between muscle and IMAT, we achieved an improvement of the agreement between the two methods, reaching a difference between the measurements of almost 12%.

In addition, partial volume issues where borderline pixels are attributed to IMAT or muscle may also contribute to error.

MRI IMAT/TA ratio and Histology adipocyte area/TA ratio were both highly correlated with BMI and waist circumference. Furthermore, MRI IMAT/TA ratio was significantly associated with age. These results confirm previous findings of a significant and strong relation between age, total body adiposity and intermuscular adipose tissue measured by mid-thigh CT (6, 22), whole-body MRI (7, 23) or ^{1}H nuclear magnetic resonance spectroscopy of the calf (24), and expands them also to a group of muscles, the erector spinae, previously only partially studied.

Some limitations of the present study should be acknowledged. First, we have a relatively small sample size due to the difficulties in selecting subjects undergoing elective surgery for medullar lumbar stenosis who did not receive steroid, pain and/or immunosuppressive medications. However, the benefit of such careful patient selection is that we are able to eliminate many potential explanatory variables with regard to the amount and distribution of the IMAT in the erector spinae muscles. Second, we elected to use high-resolution T1-weighted images to quantify IMAT in our study sample. It has been suggested that a protocol with fat-selective imaging MRI with a high sensitivity to lipid signals as described by Schick et al (25) and Goodpaster et al (26) could produce high-quality spatial maps of lipid contained within muscle and allow detecting smaller concentration of lipid within muscle tissue. However, it has also been suggested that the fat-selective imaging may make quantification of the muscle area more difficulty and obscure other structural relationships. In the T1-weighted images, it was possible to select the pixels that met our criteria and detect lipid within the muscle fascia.

In conclusion our data demonstrate that IMAT evaluated with MRI show a good degree of concordance with fatty infiltration detected by histological examination. Changing the threshold between muscle and IMAT reducing by 10% the reference of the surrounding SAT, an improvement of the agreement between the two methods was observed. However, the IMAT/TA ratio was still biased with an overestimation of percent IMAT/TA evaluated with MRI with a difference of almost 12 % between the two measurements.

These findings give further support to the use of MRI as reference noninvasive imaging method without the exposure to ionizing radiation for intermuscular adipose tissue measurement in vivo.

Acknowledgments

We thank the medical and nonmedical staff of the Department of Neurosurgery for their valuable assistance in patients recruitment and multifidus muscle biopsies during vertebral surgery. We are grateful also to the nonmedical staff of the Service of Neuroradiology for their assistance in MRI scan collection.

The contributions of the authors were as follows- MZ and TBH conceived the overall study; AR, EZ, BHG and MZ drafted the manuscript; EZ, AR and AS performed the subject screening and data collection; FP collected all MRI images and gave technical advice on MRI; AR analyzed all MRI data; AV, FC collected the histological data; AR, RM, EZ, VDF, FF performed the statistical analysis; SC, TBH, BHG, VDF, FF, RM contributed to the editing of the manuscript.

References

1. Goodpaster BH, Krishnaswami S, Resnick H, et al. Association Between Regional Adipose Tissue Distribution and Both Type 2 Diabetes and Impaired Glucose Tolerance in Elderly Men and Women. Diabetes Care. 2003; 26:372–379. [PubMed: 12547865]
2. Goodpaster BH, Thaete FL, Kelley DE. Thigh adipose tissue distribution is associated with insulin resistance in obesity and type 2 diabetes mellitus. Am J Clin Nutr. 2000; 71:885–92. [PubMed: 10731493]
3. Goodpaster BH, Krishnaswami S, Harris TB, et al. Obesity, regional body fat distribution, and the metabolic syndrome in older men and women. Arch Intern Med. 2005; 165(7):777–783. [PubMed: 15824297]
4. Gallagher D, Kuznia P, Heshka S, et al. Adipose tissue in muscle: a novel depot similar in size to visceral adipose tissue. Am J Clin Nutr. 2005; 81:903–10. [PubMed: 15817870]
5. Goodpaster BH, Carlson CL, Visser M, et al. Attenuation of skeletal muscle and strength in the elderly: The Health ABC Study. J Appl Physiol. 2001; 90:2157–2165. [PubMed: 11356778]
6. Song MY, Ruts E, Kim J, Janumala I, Heymsfield S, Gallagher D. Sarcopenia and increased adipose tissue infiltration of muscle in elderly African American women. Am J Clin Nutr. 2004; 79:874–80. [PubMed: 15113728]
7. Ross R, Leger L, Morris D, de Guise J, Guardo R. Quantification of adipose tissue by MRI: relationship with anthropometric variables. J Appl Physiol. 1992; 72:787–795. [PubMed: 1559959]
8. Mitsiopoulos N, Baumgartner RN, Heymsfield SB, Lyons W, Gallagher D, Ross R. Cadaver validation of skeletal muscle measurement by magnetic resonance imaging and computerized tomography. J Appl Physiol. 1998; 85:115–122. [PubMed: 9655763]
9. Steiger P, Block JE, Friedlander A, Genant HK. Precise determination of paraspinous musculature by quantitative CT. J Comput Assist Tomogr. 1988; 12:616–20. [PubMed: 3392263]
10. Pietrobelli A, Formica C, Wang Z, Heymsfield SB. Dual-energy X-ray absorptiometry body composition model: review of physical concepts. Am J Physiol. 1996; 271:E941–51. [PubMed: 8997211]
11. Käser L, Mannion AF, Rhyner A, Weber E, Dvorak J, Müntener M. Active therapy for chronic low back pain. Part 2. Effects on paraspinal muscle cross-sectional area, fiber type size, and distribution. Spine. 2001; 26:909–19. [PubMed: 11317113]
12. Marras WS, Jorgensen MJ, Granata KP, Wiand B. Female and male trunk geometry: size and prediction of the spine loading trunk muscles derived from MRI. Clin Biomech. 2001; 16:38–46.
13. Slend JG, Zijdenbos AP, Evans AC. A paramentric method for authomatic correction of intensity nonuniformity in MRI data. IEEE Trans Med Imaging. 1998; 17:87–97. [PubMed: 9617910]
14. Almind K, Manieri M, Sivitz WI, Cinti S, Kahn CR. Ectopic brown adipose tissue in muscle provides a mechanism for differences in risk of metabolic syndrome in mice. PNAS. 2007; 104:2366–2371. [PubMed: 17283342]
15. Greco AV, Mingrone G, Giancaterini A, et al. Insulin resistance in morbid obesity. Reversal with intramyocellular fat depletion. Diabetes. 2002; 51:144–151. [PubMed: 11756334]
16. Cinti S, Mitchell G, Barbatelli G, et al. Adipocyte death defines macrophage localization and function in adipose tissue of obese mice and humans. J Lipid Res. 2005; 46:2347–2355. [PubMed: 16150820]
17. Murano I, Barbatelli G, Parisani V, et al. Dead adipocytes, detected as crown-like structures, are prevalent in visceral depots of genetically obese mice. J Lipid Res. 2008; 49:1562–1568. [PubMed: 18390487]
18. Lin LI. A concordance correlation coefficient to evaluate reproducibility. Biometrics. 1989; 45:255–268. [PubMed: 2720055]
19. Bland JM, Altman DG. Statistical methods for assessing agreement between two methods of clinical measurements. Lancet. 1989; 8:307–310.
20. SPSS-X User's Guide. 2. Vol. 147. New York: McGraw-Hill; 1986. p. 755-63.

21. Goodpaster BH, Kelley DE, Thaete FL, He J, Ross R. Skeletal muscle attenuation determined by computed tomography is associated with skeletal muscle lipid content. J Appl Physiol. 2000; 89:104–110. [PubMed: 10904041]

22. Visser M, Kritchevsky SB, Goodpaster BH, et al. Leg muscle mass and composition in relation to lower extremity performance in men and women aged 70 to 79: the Health, Aging and Body Composition Study. J Am Geriatr Soc. 2002; 50:897–904. [PubMed: 12028178]

23. Milijkovic-Gacic I, Gordon CL, Goodpaster BH, et al. Adipose tissue infiltration in skeletal muscle: age patterns and association with diabetes among men of African ancestry. Am J Clin Nutr. 2008; 87:1590–5. [PubMed: 18541544]

24. Petersen KF, Befroy D, Dufur S, et al. Mitochondrial dysfunction in the elderly; possible role in insulin resistance. Science. 2003; 300:1140–2. [PubMed: 12750520]

25. Schick F, Machman J, Bretchtel K, et al. MRI of muscular fat. Magnetic Resonance in medicine. 2002; 47:720–727. [PubMed: 11948733]

26. Goodpaster BH, Stenger VA, Boada F, et al. Skeletal muscle lipid concentration quantified by magnetic resonance imaging. Am J Clin Nutr. 2004; 79:748–754. [PubMed: 15113711]

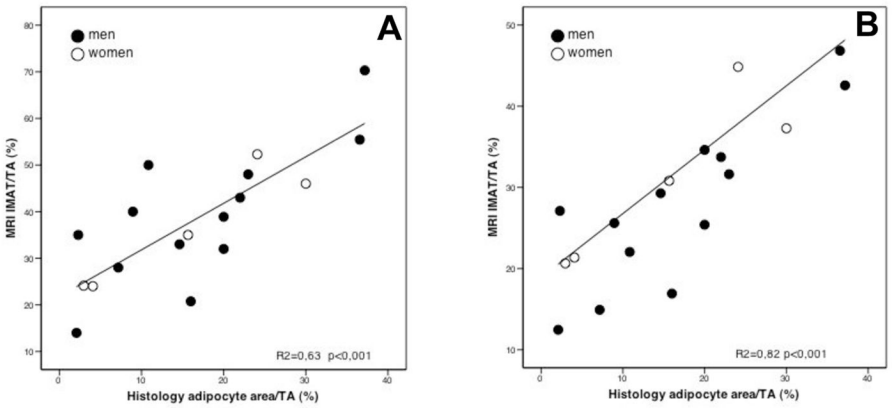

Figure 1. Simple linear correlation between IMAT/TA evaluated by MRI with 20% (A) and 10% (B) reduction of the gray level intensity referenced from the surrounding SAT and IMAT/TA evaluated by histology

MRI IMAT/TA = IMAT/TA evaluated by magnetic resonance; Histology IMAT/TA = IMAT/TA evaluated by histology;

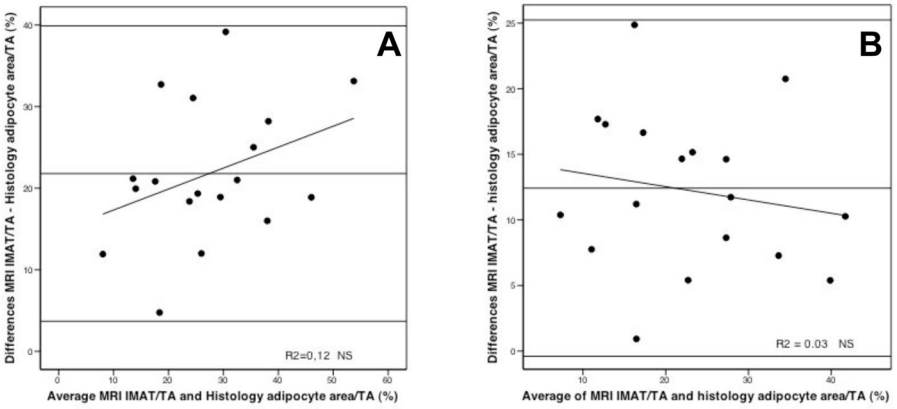

Figure 2. Difference against mean for measurements of intermuscular adipose tissue percent evaluated by histology and MRI with 20% (A) and 10% (B) reduction of the gray level intensity referenced from the surrounding SAT

Mean difference (A): 21.79%, standard deviation: 9.05, 95% Confidence interval for mean 17.54–26.05, r= 0.36, NS.

Mean difference (B): 12.42%, standard deviation: 6.41, 95% Confidence interval for mean 9.27–15.24, r=−0.17, NS.

IMAT = intermuscular adipose tissue area (measured by MRI and by histology); TA = total area (measured by MRI and by histology);

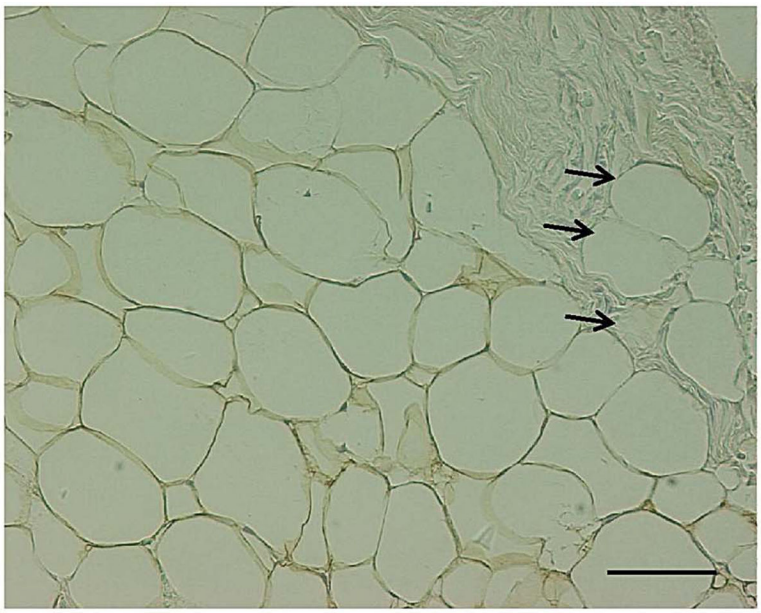

Figure 3. Intermuscular (paravertebral) adipose tissue. Perilipin immunoreactive adipocytes ([1]IHC, [2]ABC method)

Fibrosis area containing perilipin negative lipid droplets (black arrows) is visible in the right top part of the picture. Bar = 50 μm.

[1]IHC = Immunohistochemistry; [2]ABC = Avidin - Biotin Peroxidase Complex method.

Table 1

Anthropometric, body composition, MRI-measurements and histology of the study population (n =18).

Variables	x ±SD[1]	Range
Age (years)	71.3±8.0	58–81
Height (cm)	168.0±9.3	149–180
Weight (kg)	78.8±7.7	67–111.2
Waist circumference (cm)	103.2±10.51	83.5–122
DXA:		
FM (kg)[2]	27.7±7.2	18.7–40.9
FM (%)[3]	32.8±7.7	24.3–45.2
LBM (kg) [4]	54.4±4.9	36.4–80.5
ASMM (kg)[5]	25.8±2.9	14.8–37.34
MRI:		
TA (mm^2) [6]	3170.3±489.1	2104.9–4140.5
MA (mm^2) [7]	1888.3±470.5	1110.8–3102.5
IMAT (mm^2) [8] 20% (%)	1242.9±605.6	551.9–3039.7
MRI IMAT/TA[9] 20% (%)	38.2±13.9	14.0–70.30
IMAT (mm^2) [8] 10%	1065.1±529.5	449.6–2590.6
MRI IMAT/TA[9] 10% (%)	28.9±10.02	12.5–46.83
Histology:		
Histology Adipocyte area/TA section 1 (%)	16.81 ±12.66	1.08–39.2
Histology Adipocyte area/TA section 2 (%)	16.58 ± 9.56	2.28–33.1
Histology Adipocyte area/TA section 3 (%)	16.18 ±10.90	1.69–36.9
Histology Adipocyte area/TA mean (%)	16.52 ±11.10	1.68–37.2

[1] mean ± standard deviation;

[2] FM = fat mass (measured by DXA);

[3] FM (%) = fat mass percentage (measured by DXA);

[4] LBM = lean body mass (measured by DXA);

[5] ASMM = appendicular lean fat free mass (measured by DXA);

[6] TA = total area (measured by MRI);

[7] MA = muscle area (measured by MRI);

[8] IMAT = intermuscular adipose tissue area (measured by MRI);

[9] MRI IMAT/TA = IMAT/TA evaluated by magnetic resonance;

[10] Histo adipocyte area/TA = Adipocyte area on total area evaluated by histology;

Obesity (Silver Spring). Author manuscript; available in PMC 2017 January 30.

Table 2

Correlation matrix for age, anthropometric, body composition, MRI measurements and histology (n= 18 subjects) [4].

	Age	BMI	Height	Weight	Waist[5]	FM[6]	FM%[7]	MA[8]	IMAT 10% [9]	MRI IMAT/TA 20% [10]	IMAT 10% [9]	MRI IMAT/TA10% [10]	Histology adipocyte area/TA [11]
Age	1												
BMI	0.23	1											
Height	0.04	−0.36	1										
Weight	0.23	0.59[1]	0.54[1]	1									
Waist[5]	0.50[1]	0.66[2]	0.28	0.83[3]	1								
FM[6]	0.36	0.89[3]	−0.38	0.46	0.53[1]	1							
FM %[7]	0.07	0.67[2]	−0.74[3]	−0.04	0.47[1]	0.86[3]	1						
MA[8]	−0.45	−0.21	0.30	0.05	−0.26	−0.20	−0.26	1					
IMAT 20% [9]	0.52[1]	0.51[1]	0.06	0.52[1]	0.63[2]	0.42	0.14	−0.63[2]	1				
MRI IMAT/TA 20% [10]	0.58[1]	0.47[1]	−0.51	0.38	0.60[2]	0.35	0.14	−0.79[3]	0.96[3]	1			
IMAT 10% [9]	0.51[1]	0.48[1]	−0.51	0.38	0.60[2]	0.35	0.14	−0.63[2]	0.99[3]	0.95[3]	1		
MRI IMAT/TA 10% [10]	0.41	0.55[1]	−0.27	0.26	0.48[1]	0.51[1]	0.39	−0.65[2]	0.79[3]	0.83[3]	0.78[3]	1	
Histology adipocyte area/TA [11]	0.35	0.53[1]	−0.05	0.43	0.68[2]	0.45	0.24	−0.55[1]	0.79[3]	0.79[3]	0.77[3]	0.84[3]	1

[1] p< 0.05;

[2] p< 0.01;

[3] p< 0.001;

[4] data are presented as r values;

[5] Waist = waist circumference;

[6] FM = fat mass (measured by DXA);

[7] FM (%) = fat mass percentage (measured by DXA);

[8] MA = muscle area (measured by MRI);

[9] IMAT = intermuscular adipose tissue area (measured by MRI) using 20% and 10% reduction of the gray level referenced from the surrounding subcutaneous adipose tissue;

[10] MRI IMAT/TA = IMAT/TA evaluated by MRI using 20% and 10% reduction of the gray level referenced from the surrounding subcutaneous adipose tissue;

[11] Histology adipocyte area//TA = adipocyte area/TA evaluated by histology.